Molecular Crystals and Liquid Crystals
Publication details, including instructions for authors and subscription information:
http://www.tandfonline.com/loi/gmcl16

Space Charge Controlled Currents in Insulators: Detection of Virtual Anode

Martin Pope [a b] & Yedidiah Solowiejczyk [b]
[a] New York University, Chemistry Department
[b] Radiation and Solid State Laboratory
Version of record first published: 21 Mar 2007.

To cite this article: Martin Pope & Yedidiah Solowiejczyk (1975): Space Charge Controlled Currents in Insulators: Detection of Virtual Anode, Molecular Crystals and Liquid Crystals, 30:3-4, 175-200

To link to this article: http://dx.doi.org/10.1080/15421407508083430

Mol. Cryst. Liq. Cryst., 1975, Vol. 30, pp. 175–200

Printed in Holland

Space Charge Controlled Currents in Insulators

Detection of Virtual Anode

MARTIN POPE†‡ and YEDIDIAH SOLOWIEJCZYK‡§

New York University, Chemistry Department† and Radiation and Solid State Laboratory‡

(*Received August 7, 1974; in final form December 19, 1974*)

Using tetracene crystals provided with hole injecting contacts (CuI(s) and $Ce(SO_4)_2$(aq)) we have located the position of the virtual anode x_m (potential maximum) within the crystal and have studied its voltage dependence. For this purpose, we used the triplet and singlet excitons as tracers, making particular use of the characteristic response of these excitons to an external magnetic field. The voltage dependence of x_m follows that predicted by the simplified form of the exact theory of Sinharay and Meltzer. It appears that x_m lies within the crystal for all voltages up to the saturation voltage. It is shown that a photoenhanced current will be produced not only by detrapping deep in the interior of the crystal, but by detrapping in the vicinity of the virtual anode x_m.

I INTRODUCTION

The flow of a steady unipolar current through an insulator containing bulk trapping sites, and provided with one injecting contact and one neutral contact has been the subject of many theoretical studies.[1,2,3] In the special case of organic insulators, the most widely used theory is that developed initially by Rose[4] and Lampert[2] for space charge limited currents (SCLC) and applied by Mark and Helfrich[2,5,6] (MH) to organic insulators. This theory (MH theory) is relatively simple and has been successful in helping to interpret the current-voltage (J–V) behavior in terms of trapping densities and the trap energy level distribution. The MH theory is based in part upon the postulate of an infinite supply of carriers at the injecting electrode (an ideal ohmic contact) and the neglect of the diffusion current as compared with the drift current. If one solves the general equation of current flow

§ This work is based on the dissertation prepared by Y. Solowiejczyk in partial fulfillment of the requirements of the Ph.D. in Physics at New York University.

through an insulator, using more realistic boundary conditions that recognize the finiteness of the reservoir of carriers at the injecting electrode, and including the diffusion current,[3,7,8] then it is quite difficult to obtain a convenient expression for the $J-V$ dependence. For the sake of simplicity, the more exact theory will be referred to herein as the SM theory merely because we shall be using a particular form proposed by Sinharay and Meltzer.[7,8] As might be expected, the results of the MH theory and the SM theory are in fair agreement for the region of the crystal that is far removed from the injecting contact, and over that limited voltage range for which the voltage is low enough so that the current is far from saturation but not so low that diffusion currents are important over most of the crystal. If as is the case in this work, the applied voltage traverses a range that includes the diffusion current and the saturation current, and if one is studying phenomena that take place close to the injecting electrode, then the MH theory will not be adequate, and an exact theory must be used. Whereas the MH theory employs SCLC, the more exact SM theory employs the concept of a current that is controlled both by the size of the injecting reservoir and by space charge.

We report here an experimental study of the $J-V$ dependence of a tetracene crystal provided with a CuI hole injecting contact. By using singlet and triplet excitons to probe the trapped carrier distribution, and by using an external magnetic field, we provide evidence for the existence within the crystal of a potential maximum that moves towards the anode with increasing voltage. In some cases the potential maximum is detected at a distance 10μ from the geometrical anode in a crystal that is 180μ thick. This work is a continuation and amplification of previously reported studies.[9,10] The MH theory is unsuited for processes that take place near the injecting electrode. An approximate form of the SM theory, also derived by Sinharay and Meltzer[7,8] will be used to rationalize the observed results.

Consider the case of an insulator containing no chemical impurities, no thermally generated carriers, and provided with a hole-injecting CuI(s) contact and an opposing evaporated Ag contact. As is explained in a particularly clear fashion by Mott and Gurney[1] and by Frank and Simmons,[11] even in the absence of an applied field, holes can be thermionically injected into an insulating crystal, as a result of which a concentration gradient of holes will be set up in the region near the contact. This concentration gradient produces a diffusion current flowing into the crystal that is opposed by electrical restoring forces between the carriers and the injecting electrode. One electrical restoring force consists of the short-range (~ 100 Å) image force that can be large ($\sim 10^6$ V/cm) and is therefore usually the dominant field for distances within 100 Å of the electrode. A longer range force is that generated by the presence on the injecting electrode of the countercharge to the injected carriers. This longer range force is more comparable to the

external electric field. We shall be concerned only with internal fields that are comparable in size to the external field.

If an external field is applied that forces the carriers away from the injecting electrode, then, since the injected carriers are in addition always acted upon by the restoring force towards the injecting electrode, there can be a point x_m inside the crystal where for a particular range of applied voltage, the two opposing forces balance, and the net internal field $E = 0$. Near the injecting contact, there is therefore a potential well that extends to x_m, for the appropriate range of applied voltage.[3] This is shown in Figure 1 where the injecting contact is at $x = 0$ and the potential well lies between $x = 0$ and $x = x_m$.

The steady state current flow, J, of positive charge in one dimension through the insulator can be expressed as

$$J = n_f e\mu E - \mu kT \frac{dn_f}{dx} \tag{1}$$

where n_f is the density of free carriers at x, and μ, k, T, e are the carrier mobility, Boltzmann's constant, absolute temperature, and electronic

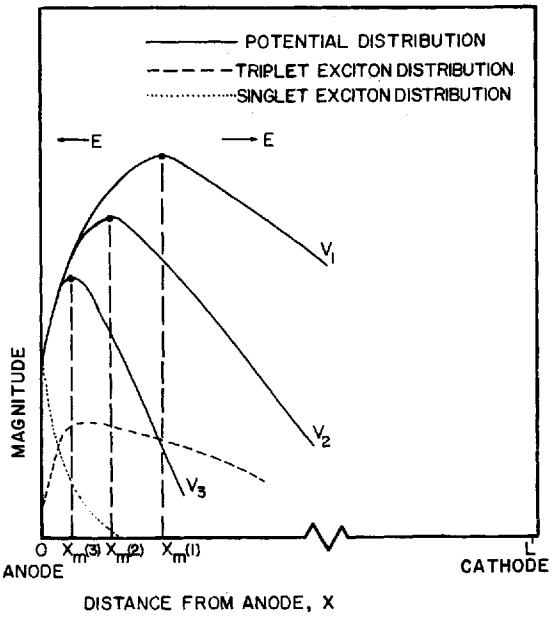

FIGURE 1 Qualitative relative spatial distribution of the internal electric potential, the triplet exciton density and the singlet exciton density in a tetracene crystal of thickness L. The internal potential is shown for various applied electric fields. E is the internal electric field, V_1, V_2, V_3 are series of applied voltages where $V_3 > V_2 > V_1$. Note that E changes direction at the potential maximum x_m.

charge, respectively; E and n_f are generally functions of x. The term containing E in equation (1) is called the drift current and the term containing kT is referred to as the diffusion current. From equation (1) it may be seen that at x_m, where $E = 0$, the observed current is carried entirely by diffusion; where E is large, diffusion will play a minor role. The point x_m acts as a virtual anode for the region $x_m \lesssim x \lesssim L$, where L is the crystal thickness. Additional relations are:

$$\frac{dE}{dx} = \frac{n_{\text{total}} e}{\varepsilon\varepsilon_0} \quad \text{Poisson's Equation} \tag{2}$$

where

$$n(\text{total}) = n(\text{free}) + n(\text{trapped}) = n_f + n_t$$

and

$$V_{\text{applied}} = -\int_0^L E\, dx \tag{3}$$

From equations (1), (2), (3), and boundary conditions that provide for a finite, constant density of carriers at the anode ($x = 0$) and cathode ($x = L$), Sinharay and Meltzer[7,8] (SM), were able to derive a useful approximate expression giving x_m, for the trap-free case, as a function of the observed current and the given anode concentration of free carriers (n_a). This relation is:

$$x_m = \frac{2\mu kT}{b^{3/2}} \left\{ \frac{b^{1/2}}{J^{1/3}} - \frac{1}{n_a^{1/2}} \right\} \tag{4}$$

where

$$b = \frac{1}{1.018} \left[\frac{\mu^2 e^2 kT}{2\varepsilon\varepsilon_0} \right]^{1/3} \tag{5}$$

At low external fields, x_m lies deep inside the crystal, and as the external field is increased, x_m moves towards the anode. When $x_m = 0$, the virtual anode is identical with the geometric anode, and for still higher applied fields, x_m leaves the crystal and the current approaches saturation. The movement of x_m with applied field is shown schematically in Figure 1.

II CURRENT-VOLTAGE (J–V) BEHAVIOR

With this brief introduction we will now examine the experimental results which were obtained on four crystal samples. In Figure 2 is shown a J–V curve for a tetracene crystal provided with a hole-injecting CuI contact. In

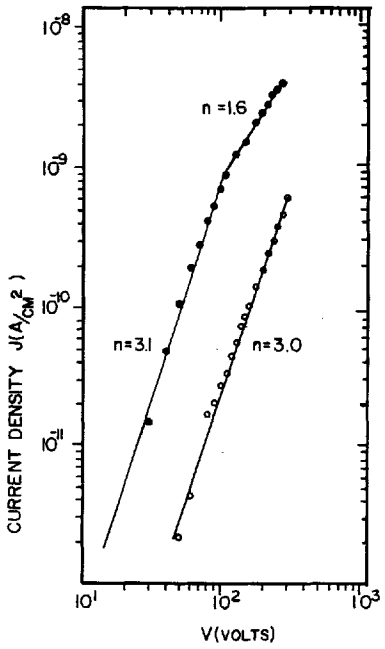

FIGURE 2 Current-voltage (J–V) dependence for a tetracene single crystal in absence (○) and presence (●) of highly absorbed light ($k = 4 \times 10^4$ cm^{-1}) of intensity $I_0 \approx 10^{14}$ cm^{-2}s^{-1}. The power n appears in the relation $J \propto V^n$. CuI anode, evaporated Ag cathode. Crystal thickness $L = 75\mu$.

the dark, the J–V dependence is of the type $J \propto V^n$, $n \simeq 3$. This response is typical of a SCLC[2] with a trap distribution that is exponential in energy. In the presence of light, the current is increased (photoenhancement) and two voltage dependencies are observed; up to about 14,000 V/cm, $J \propto V^{3.1}$ and beyond this field, $J \propto V^{1.6}$. At lower fields, the J–V dependence is still characteristic of a trap distribution that is exponential in energy.[2] The absorption of light apparently has very little effect on the value of n whereas according to Helfrich[6] the value of n should approach 2 as photoenhancement dominates. At higher fields the photoresponse is reminiscent of a contact that is saturating. The enhanced current produced by the light can, in principle, be attributed to an increase in the carrier concentration in the anode reservoir or to an increase in the ratio of free to trapped carriers in the bulk, or to both. It is at this point in the interpretation of the photoresponse that there is a significant qualitative difference between the MH theory and the more exact theory. Helfrich[6] states that if highly absorbed light is used to illuminate an ohmic contact, then according to the MH theory, the photoenhancement can only be due to detrapping of carriers in the bulk, since the

contact is assumed to have an infinite reservoir of carriers in the dark. However, an ideal ohmic contact is seldom realized, so the conclusion of Helfrich[6] must be modified; the more exact theory must be used to determine the effect of highly absorbed light. The exact theory shows[2] that at a given voltage, the observed dark current is a function of the free carrier concentration at the anode, if this concentration is less than $\sim 10^{16}/\text{cm}^3$ for a 50μ crystal of $\varepsilon = 11$; this is almost invariably the case with organic insulating crystals provided with the injecting electrodes that have been described in the literature. Highly absorbed light can therefore increase the concentration of free carriers at x_m if the anode concentration is increased and thereby cause an increase in the observed current, without necessarily affecting the ratio of free to trapped carriers in the bulk of the crystal to a significant degree.

III ACTION SPECTRUM OF THE PHOTOENHANCED CURRENT

We now examine the action spectrum for the photoenhanced current; this is shown in Figure 3a,b for applied fields of 5,300 (40 V), 13,000 (100 V) and 27,000 (200 V) V/cm respectively. The absorption spectrum for b polarized light is given in Figure 3a. There are three striking features in these figures. At wavelengths lying within the main absorption region of tetracene, the photoenhancement is antibatic (inversely proportional to the absorption coefficient); secondly, in the long wavelength tail of the main absorption band, there is a large enhancement peak that does not correspond to any feature in the absorption spectrum; finally, the position of the long wavelength peak is field-dependent, moving towards shorter wavelengths as the field is increased. Effects similar to these have been observed previously.[12,13] The interpretation of these qualitative features is as follows: the antibatic photoenhancement response in the main absorption region is evidence that detrapping in the bulk is a dominant mechanism. Thus, the more weakly absorbed the light, the greater the penetration depth, and hence the greater the degree of detrapping. In our particular case the detrapping can be effected by both singlet excitons and triplet excitons; for wavelengths $440 < \lambda < 510$ nm the triplet exciton dominates the detrapping process. This last conclusion is based on the following: the diffusion length of the singlet exciton is about 100 Å[14] because its lifetime with respect to fission into two triplet excitons is about 2×10^{-10} sec.[15,16] On the other hand, the diffusion length of the triplet exciton is about 0.4μ.[17,18,19] Mulder[20] has shown that if the distance that an exciton must travel in order to be effective in a dominant process (such as detrapping) is large compared with its diffusion length, then the action spectrum of that process will vary strongly with the absorption depth of the light. If on the other hand the distance the exciton must travel is small

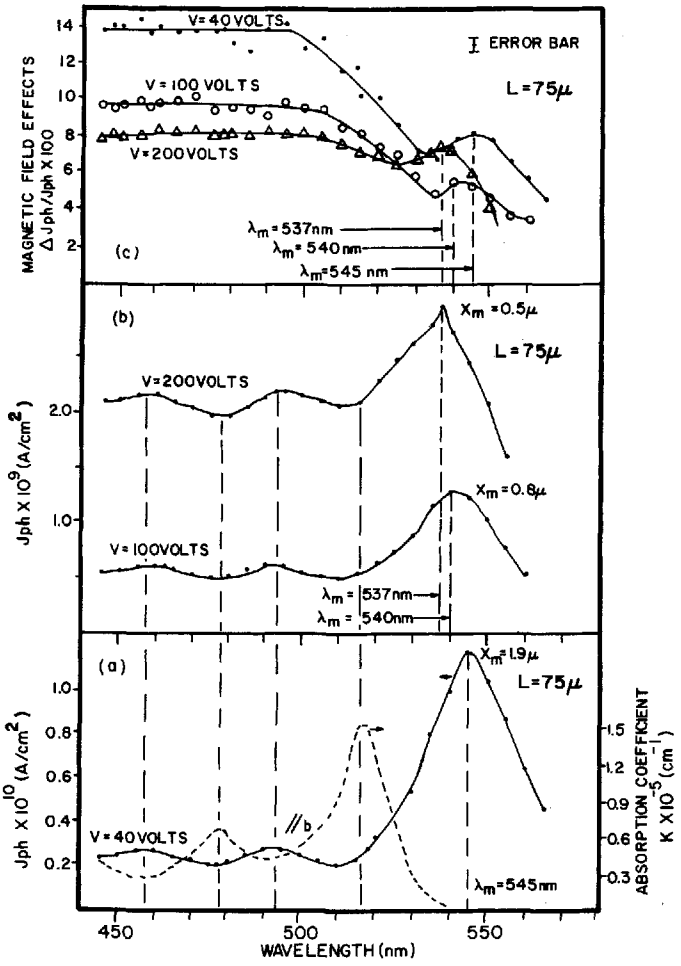

FIGURE 3a Absorption spectrum of tetracene single crystal $\|b$ axis[34] (dashed curve, ordinate to the right). Photoenhanced current (J_{ph}) action spectrum for an applied voltage of 40 volts (solid curve, ordinate on left). Crystal thickness $L = 75\mu$.

FIGURE 3b Photoenhanced current (J_{ph}) action spectrum for 100 and 200 volts applied to tetracene crystal. $L = 75\mu$.

FIGURE 3c Action spectrum of effect of an external magnetic field (4000G applied in the ab plane at the resonance position of 30° with respect to b axis) at various applied voltages. $\Delta J_{ph}/J_{ph} \equiv \{J_{ph}(\mathbf{H}) - J_{ph}(\mathbf{0})\}/J_{ph}(\mathbf{0})$, where J_{ph} is the current in the presence of light. **H** and **0** refer to magnetic field on and off respectively. For (a), (b), (c), $L = 75\mu$. constant light intensity $I_0 \approx 10^{14}$ cm^{-2}s^{-1}, CuI anode, Ag cathode. For definition of λ_m, J_{ph}, and x_m, see text.

or commensurate with its diffusion length, then the action spectrum for the process will vary weakly with the absorption depth of the light. The comparatively weak dependence of the photoenhanced current on the absorption depth (compare the peak to valley ratio in the photocurrent with that in the absorption spectrum) therefore would ordinarily indicate that the main body of trapped carriers is within a few exciton diffusion lengths of the anode. Since the main body of trapped charge lies closer to the anode than to the cathode, then the absorption depth of the light of wavelength λ_m in Figure 3a,b should correspond in some way to the region of coincidence of the centers of gravity of the excitons and the trapped charge. This distance is in no case less than 0.4μ. If the singlet exciton were to be mainly responsible for the photoenhancement, one would expect the action spectrum for photoenhancement to vary as strongly as does the absorption spectrum[20] because the diffusion length of the singlet exciton is less than 1/50 of the distance from $x = 0$ to the center of gravity of trapped charge. Since the position of the center of gravity of trapped charge is commensurate with the diffusion length of the triplet exciton, and the antibatic response is weakly dependent on k, one would conclude that the triplet exciton is mainly responsible for detrapping. There is however another possible explanation for the weakly antibatic response; namely, that excitons are simultaneously injecting charge at the surface and detrapping charge deeper in the crystal. Since the charge injection would show a symbatic response and detrapping an antibatic response, the overall effect would be a weakened resultant. Fortunately, the magnetic field (**H**) dependence of the photoenhancement (Section IV) shows that the triplet exciton is mainly responsible for the antibatic response.

IV EFFECT OF MAGNETIC FIELD (H) ON THE PHOTOENHANCED CURRENT

As was postulated by Swenberg and Stacy[21] and demonstrated by Geacintov, *et al*[22] and Pope, *et al*,[15] the low fluorescence efficiency of tetracene crystal ($\sim$0.002 at room temperature) is due to an accidental near-degeneracy of the singlet level ($\sim$2.4 eV) and an energy that represents the sum of two triplet exciton energies ($\sim$2.56 eV). Because of this near-degeneracy, the singlet exciton can fission at room temperature into two triplet excitons in a spin-allowed, radiationless, activated process that effectively depletes the population of singlet excitons. The application of an external magnetic field of about 4000G can diminish the fission efficiency by as much as 40%; the subsequent increase in the concentration of singlet excitons is easily detected as a 40% increase in the fluorescence efficiency of the crystal at 4000G. More importantly, the change in fluorescence efficiency with magnetic field **H** is not

monotonic with **H**. For $0 \lesssim \mathbf{H} \lesssim 400$G, the fluorescence efficiency first decreases upon the application of a magnetic field, reaching a minimum of -7% at 250G, after which the fluorescence efficiency increases, passing through 0 at about 400G; it then becomes positive, saturating at $+40\%$ at 4000G. This inversion in the sign of the magnetic effect is a characteristic signature of singlet excitons.

As for the triplet excitons, they too have a characteristic signature that is usually revealed in delayed fluorescence (DF) studies. Thus, in anthracene,[23] the algebraic sign of the effect of **H** on the DF produced by triplet–triplet (T–T) fusion also exhibits an inversion but in the opposite direction to that shown by fission in tetracene, i.e. the DF in anthracene is larger for $0 < \mathbf{H} <$ 400G. In tetracene, T–T fusion to form a singlet exciton is not observed at room temperature because the singlet so produced immediately fissions back again into two triplets. However, at 4000G, there is a net loss of about 2% and for $\mathbf{H} < 400$G there is a 0.2% net increase in the triplet population because of the **H** dependence of the fission process;[15] this change in triplet population can be identified because it is qualitatively the inverse of the change in singlet population.

Not only does an external **H** decrease the overall efficiency of the T–T fusion process, it decreases the efficiency of the interaction of a triplet exciton with such paramagnetic species as free radicals[24] and trapped charge.[25] There is also a characteristic **H** dependence for these triplet exciton quenching processes. As distinct from T–T fusion, the triplet-radical and triplet-trapped carrier (T–n_t) interaction decreases monotonically with increasing **H**, reaching about -7% for anthracene before saturating. For tetracene, the same process has been observed.[25] It is thus easy to distinguish the T–T from the T–n_t interaction, using an external magnetic field as a probe. It should be kept in mind that the experimental manifestation of the effect of an external **H** on exciton interactions in tetracene (or in other crystals) need not be confined to changes in fluorescence intensity. Thus, if the T–n_t interaction is decreased, then the carrier detrapping process is correspondingly diminished; this is usually observable as a decrease in photoenhancement. However, due to the possible presence of intricately coupled processes within the crystal, the algebraic sign of the **H** effect is not an invariant; nevertheless, the presence or absence of inversions in the algebraic sign of the **H** effects is distinctive.

In the experiments to be discussed herein, we shall be confining our attention to changes in electrical conductivity produced by excitons, and the effect of a magnetic field thereon. This change is indicated in the form $\Delta J_{ph}/J_{ph}(\mathbf{0}) \equiv \Delta J_{ph}/J_{ph}$ where $\Delta J_{ph} \equiv J_{ph}(\mathbf{H}) - J_{ph}(\mathbf{0})$; $J_{ph}(\mathbf{H})$, $J_{ph}(\mathbf{0})$ are respectively the photoenhanced currents in the presence and absence of a magnetic field. In interpreting the **H** effects in tetracene, we must keep in

mind the fact that in the steady state condition the triplet population $[T]$ is $>10^5[S]$;[10] this relationship is a consequence of the fact that the ratio $[T]/[S] \simeq \tau_T/\tau_S$ where τ_T is the lifetime of the triplet exciton and τ_S is the lifetime of the singlet exciton with respect to fission. Since $\tau_T \simeq 10^{-4}$s,[18] and $\tau_S \simeq 10^{-10}$s,[16] one has $[T] \simeq 10^6[S]$, where $[S] \equiv$ singlet exciton density.

However, in addition to the concentration of excitons, the exciton-trapped carrier interaction coefficient must be taken into consideration in order to evaluate the relative effectiveness of the singlet and triplet excitons in detrapping carriers. Unfortunately, there are no data for the singlet exciton-trapped carrier interaction coefficient (γ_{St}) for tetracene. We shall therefore use the data for anthracene. In anthracene, the singlet exciton-trapped carrier (S–n_t) interaction coefficient γ_{St} is[27] about 10^{-8} cm^{3}s^{-1} and the triplet exciton-trapped carrier (T–n_t) coefficient γ_{Tt} is[28] about 10^{-11} cm^{3}s^{-1}. Using these relative anthracene values for tetracene, one therefore obtains the ratio $\gamma_{St}[S]/\gamma_{Tt}[T] \simeq 10^{-3}$, which is a measure of the overall effectiveness of the singlet exciton as a detrapping agent based on its concentration. A point may be raised about the role of carrier lifetime and carrier gain in affecting the observed currents.[35] To begin with, we are not generating hole-electron pairs inside the crystal. Secondly, since we are using ohmic contacts, there is essentially no role to be played by excitons insofar as increasing the rate of injection is concerned. As for detrapping, a carrier detrapped thermally or optically has the same lifetime, so it is entirely permissible to compare the singlet detrapping rate with the triplet detrapping rate without considering carrier lifetimes. If the singlet exciton is to have any noticeable effect in the presence of the triplet exciton, it must therefore be a consequence of its greater energy, because both the T–n_t and S–n_t processes are highly allowed.

Summarizing, one should keep in mind that in tetracene, an external magnetic field enhances the singlet exciton fission at low field ($\mathbf{H} < 400$G) to a maximum of about 7% and represses the fission at high fields ($\mathbf{H} > 2000$G) to a maximum of about 40%. Concurrently, the triplet exciton population is altered in an opposite sense, increasing by a maximum of about 0.2% for $\mathbf{H} < 400$G and decreasing by a maximum of 2% for $\mathbf{H} > 2000$G. Thus, if there is an inversion in the sign of $\Delta J_{ph}/J_{ph}$ as $\mathbf{H}$ is increased from 0 to 4000G, then singlet excitons are certainly involved; if the magnitude of the effect is less than 2%, then it is also possible that only triplet excitons are involved, since the $[T]$ population change is the inverse of the $[S]$ population change, reaching a maximum of -2% when singlet fission is aborted. If there is no inversion in the sign of $\Delta J_{ph}/J_{ph}$ as $\mathbf{H}$ is increased from 0 to 4000G, and if $\Delta J_{ph}/J_{ph}$ is a monotonic function of $\mathbf{H}$, then the triplet exciton is dominating the photoenhancement process.

It is thus possible to distinguish between singlet excitons and triplet excitons by examining the $\mathbf{H}$ dependence of J_{ph}. This is shown in Figure 4b

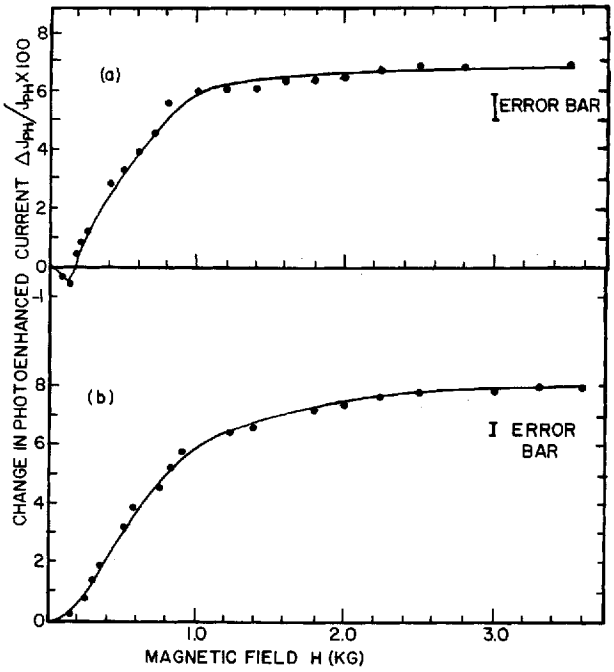

FIGURE 4 Effect of an external magnetic field (at resonance position in the *ab* plane at an angle of 30° with respect to *b* axis) on the photoenhancement current (J_{ph}) for 200 volts applied. (a) Incident light intensity, $I_0 \approx 10^{14}$ cm^{-2}s^{-1}, $\lambda = 535$ nm $\|b$ axis, $l_a = 1/k = 0.4\mu$. (b) Incident light intensity, $I_0 \approx 10^{14}$ cm^{-2}s^{-1}, $\lambda = 510$ nm $\|b$ axis, $l_a = 1/k = 0.13\mu$, $L = 75\mu$, CuI anode and Ag cathode.

for one particular wavelength, 510 nm, where the typical monotonic response of triplet excitons is clearly evident. Note however that $\Delta J_{ph}/J_{ph}$ is positive, instead of negative. This reversal (see paragraph 3, Section IV) is highly significant and will be discussed in detail in Section VII. The same **H** dependence is found at several other wavelengths between 440–510 nm; we thus conclude that triplet excitons are mainly responsible for the photoenhancement in this wavelength region. This does not mean that singlets do not detrap; it means that the triplet excitons dominate the detrapping process.

V APPEARANCE OF THE PHOTOENHANCEMENT PEAK AT $\lambda = \lambda_m$

Consider now the large photoenhancement peak at λ_m in the long wavelength tail of the action spectrum shown in Figure 3a,b. Certainly there is nothing in the absorption spectrum at λ_m to explain this peak, and its electric field dependence indicates that there is apparently an interplay between a field

dependent trapped charge distribution and the exciton distribution produced by the absorbed light. Such an explanation has in fact been used by Bauser and Ruf[12] to rationalize similar peaks that they observed in their studies in anthracene provided with an iodine contact. Bauser and Ruf used the MH theory and obtained good agreement between the predictions of the MH theory and experiment. On the other hand, based on the interpretation given by Fox[10] and Pope, *et al*[9] of their results on tetracene, the peak at λ_m indicates the position of the potential maximum or virtual anode at a distance x_m within the crystal; that is, $x_m \simeq 1/k_m$, where k_m is the absorption coefficient at λ_m. It is also possible to justify the appearance of the peak at λ_m without resorting to the use of x_m or the Bauser and Ruf theory. One could imagine for example that the same excitons both assist in the injection of charge at the electrode and in the detrapping of charge in the bulk.[26] If this were the case, then there certainly would be an optimum absorption depth that would facilitate both the injection and detrapping; if the trapped charge distributions were field dependent, then the peak would be field dependent. However, these alternate mechanisms cannot explain the observed magnetic field dependence of the peak $\Delta J_{ph}/J_{ph}$ at λ_m, as will be shown below.

The experimental results are as follows: at $\lambda = \lambda_m$ for any particular applied field, there is a distinctive peak in the action spectrum for $\Delta J_{ph}/J_{ph}$, as is shown in Figure 3c. At this peak, one sees the characteristic signature of the singlet exciton detrapping process. This is shown in Figure 4a where the inversion in the sign of the magnetic field effect and the large overall magnitude of the H effect ($>2\%$) are evident. However, the small size of the inversion ($<1\%$) and the appearance of the cross-over at 200G instead of 400G indicate that triplet exciton detrapping is taking place concurrently, to a comparable extent. In order for singlet exciton detrapping to be comparable with triplet exciton detrapping, the greater energy of the singlet exciton must be the dominant feature, in view of the overall ineffectiveness (10^{-3}) of the singlet exciton based on its concentration. In addition, the population of trapped carriers available only to the singlet exciton would have to be ~ 1000 times greater than that available to the triplet exciton in order to overcome the 1000 fold superiority of the triplet exciton. A close examination of the alternate mechanisms[12,26] shows that they do not rely on an energetic distribution of trapping levels for the appearance of the peak in the photoenhancement action spectrum at λ_m, but instead, rely on a voltage dependent spatial distribution of trapped carriers. There is therefore nothing in either theory that provides an opportunity for the singlet exciton to make use of its superior energy. This does not mean that these mechanisms are physically defective. It just means that in our case, where we work with thinner ($\lesssim 180\mu$) crystals, the surface region is more important than in the work of Bauser and Ruf who worked with thicker crystals ($>700\mu$).

In our case, the photoenhancement is decidedly antibatic thus showing that photoenhancement due to detrapping is more important than enhanced carrier injection.

As will be argued in greater detail, we conclude that there is a local, field dependent, potential barrier at $x_m \simeq 1/k_m$, and that the peak at λ_m marks a point x'_m that is actually slightly $< x_m$ by several hundred Å at which point the singlet excitons, with their superior energy, can photoinject carriers over the potential barrier at x_m shown in Figure 1, whereas the triplet excitons find it very difficult to do so. It must be kept in mind that in the MH SCLC theory, any increased injection of carriers over the barrier at x_m into the crystal would have no effect on a SCLC current since the contact has been assumed to contain an infinite reservoir of charge. However, in the more exact theory, the space charge controlled current is also a function of the free carrier concentration at x_m, and will increase if the free carrier concentration at x_m increases.

VI THEORETICAL DEPENDENCE OF x_m ON J_{ph}

If $1/k_m$ is to be interpreted as corresponding to x_m, then the J dependence of $1/k_m$ should be given by equation (4). This is shown in Figure 5, where in

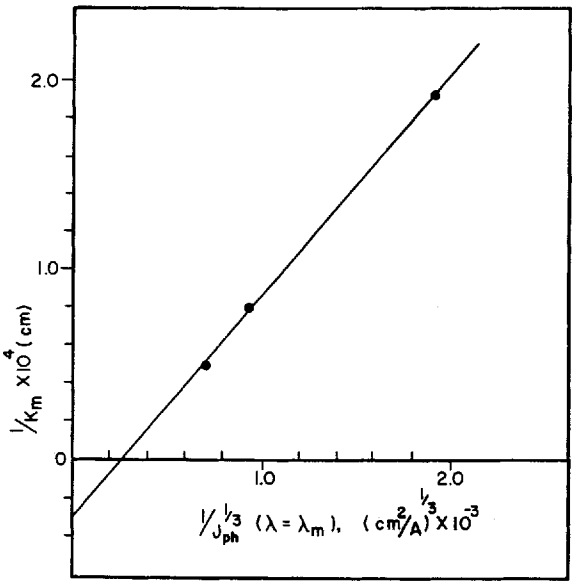

FIGURE 5 Plot of experimental value of $1/k_m$ as a function of $1/J_{ph}^{1/3}$ ($\lambda = \lambda_m$). k_m and λ_m are the absorption coefficient and wavelength of light at the long wavelength peak in the action spectrum of the photoenhanced current. See Figure 3a,b. $L = 75\mu$, CuI anode, and Ag cathode.

accordance with the form of equation (4), a plot of $1/k_m$ against $1/J_{ph}^{1/3}$ ($\lambda = \lambda_m$) should yield a straight line; J_{ph} ($\lambda = \lambda_m$) is the total current at the given voltage and at $\lambda = \lambda_m$. This has been found to be the case with all the crystals and all the injecting electrodes we have studied. As may be seen from equation (4), important crystal parameters can in principle be calculated from the experimental fit of the data. However, we are presently limited by the fact that the Sinharay and Meltzer (SM) theory was derived for a trap-free crystal. The modification of the SM theory to include simple trapping in a single discrete level is straightforward;[10] it amounts to merely replacing ε by ε' in equation (5) where $\varepsilon' = \varepsilon\theta$ and $\theta = n_f/(n_f + n_t)$. Using the following values for the physical constants of tetracene: $\mu = 0.5$ cm^2 $V^{-1}S^{-1}$,[29] $\varepsilon = 3.8$,[29] and the value $m = 1.4 \times 10^{-7}$ for the slope of the curve shown in Figure 5, one obtains:

$$\begin{aligned} b(\text{experimental}) &= 2.9 \times 10^{-14}\ (\text{cm}^5\ \text{coul}^2\ \text{s}^{-2})^{1/3} \\ b(\text{theoretical}) &= 3.5 \times 10^{-16}\ (\text{cm}^5\ \text{coul}^2\ \text{s}^{-2})^{1/3} \\ b(\text{exp})/b(\text{th}) &= \theta^{-1/3} = 83;\ \theta = 1.9 \times 10^{-6} \end{aligned} \tag{6}$$

$$\frac{b^{1/2}\exp}{(J_{ph}^{1/3})_{x_m=0}} = \frac{1}{n_a^{1/2}(\text{free})};\ n_a(\text{free}) = 4.5 \times 10^8\ \text{cm}^{-3};$$

$$n_a(\text{total}) \simeq n_a(\text{trapped}) = 2.5 \times 10^{14}\ \text{cm}^{-3}$$

The values obtained in equation (6) are approximate because the actual trapping levels in tetracene are not monoenergetic.

In addition to the prediction of the linearity of a plot of $1/k_m$ against $1/J_{ph}^{1/3}$ ($\lambda = \lambda_m$), it is possible[9] to use the SM theory to derive a relation similar to that first given by Bauser and Ruf,[12] namely, $k_m L$ = constant, where L is the crystal thickness. This is done[9] by substituting for J_{ph} ($\lambda = \lambda_m$) in equation (4) the SCLC approximation[2] $J_{ph} = (9/8)\mu\varepsilon\varepsilon_0\theta V^2/L^3$. Keeping in mind that $b(\text{exp}) = b(\text{th})\theta^{-1/3}$, and that we have postulated that $x_m \simeq 1/k_m$, one obtains

$$k_m L = (10V)^{2/3}(1 + k_m/k_m^0) \tag{7}$$

where $k_m^0 = b_{exp}^{3/2} n_a^{1/2}/2\mu kT$ is obtained from the plot of equation (4). As may be seen from equation (7), if V is constant, then $k_m L$ is constant if $(1 + k_m/k_m^0)$ is fairly constant; this turns out to be approximately the case. In Table I, one sees in columns B and D the measured and calculated (using equation (7)) values respectively of $k_m L$. Despite the differences in the electrode material, the agreement between the calculated and measured values is as good as one should expect from the approximate SM theory, considering also the assumptions made in deriving equation (7). Bauser and Ruf[12] did not give sufficient data in their paper to enable us to check their

TABLE I

				A	B	C	D
Crystal Number	Electrode Material	Voltage (Volts)	Thickness $L(\mu)$	k_m (μ^{-1})	k_mL	$1/k_m^0$ (μ)	$(10V)^{2/3}(1 + k_m/k_m^0)$
21	CuI	20	98	1/1.3	77	0.6	50
		40		1/0.75	130		97
		80		1/0.45	218		193
22	CuI	40	75	1/1.9	40	0.3	63
		100		1/0.75	100		139
		200		1/0.45	167		266
40	$Ce(SO_4)_2$	40	180	1/7.5	24	2.2	70
		80		1/0.75	240		326
		100		1/0.45	400		588

results with equation (7); using the data in Table I and the theory of Bauser and Ruf, it was not possible to get any better agreement among the crystals of different thickness (at constant voltage) than is obtained using equation (7). The interesting feature of equation (7) is that it does not take into consideration the exciton distribution, which is a vital part of the Bauser and Ruf theory.

VII RATIONALIZATION OF THE POSITIVE VALUE OF $\Delta J_{ph}/J_{ph}$ FOR $\lambda < \lambda_m$

Let us now return to the problem of the apparently paradoxical, relatively large ($\sim 13\%$) *positive* value of $\Delta J_{ph}/J_{ph}$ that characterizes the action spectrum of photoenhancement for $\lambda < \lambda_m$; this photoenhancement has been attributed herein to triplet exciton detrapping and since **H** *reduces* the T–n_t interaction, the observed magnetic effect, $\Delta J_{ph}/J_{ph}$, should have been *negative*. This paradox can be resolved by involving the potential maximum at x_m and the potential well lying between $0 \lesssim x \lesssim x_m$. The question that must be posed is how can a *reduction* in the T–n_t interaction lead to an *increase* in the photoenhancement? We propose that for the important region $x < x_m$, the detrapping of carriers is effective in increasing the current only if the detrapped carriers can enter the region $x > x_m$. Since there is a potential barrier at $x = x_m$, only those carriers with sufficient kinetic energy to surmount the barrier can enhance the current. A corollary to our proposition that the singlet exciton produces the photoenhancement peak at λ_m is that there must be an opportunity for the greater energy of the singlet exciton to manifest itself. In other words, the range of the detrapped carrier must be significantly greater if it starts out with an additional 1.2 eV

of kinetic energy. This is not a trivial requirement; in view of the narrowness of the lowest conduction band in organic insulators, the maximum kinetic energy that can be imparted to a carrier in this band is $\lesssim kT$. It thus appears that there must be a higher, broader conduction band or some other mechanism for increasing the range of the detrapped carriers, and that the triplet exciton is not as effective in utilizing these channels as is the singlet exciton. Furthermore, the detrapping must take place close enough to x_m to permit the excited carrier to escape over the barrier (as if it were photoinjected) while it still has excess kinetic energy because the internal electric field in the region $x < x_m$ is in the opposite direction to that required to assist the carrier over the potential barrier (see Figure 1). So it is virtually at x_m that the detrapping is most important.

Summarizing, we have proposed that it is the concentration of free carriers at the virtual anode x_m that determines the magnitude of the current, and that the triplet exciton can be most effective in increasing the free carriers concentration at x_m by detrapping carriers at x_m. If we assume as a first approximation that the photoenhanced concentration of free carriers at x_m is much larger than that present during the dark conduction, we can say that

$$(n_f)_{x_m} = \frac{\gamma_{Tt}([T][n_t])_{x_m}}{k_t} \tag{8}$$

where k_t is the retrapping rate. Equation (8) implies a linear light intensity dependence for the photoenhanced current and the observed power dependence on the light intensity is 0.8. Since not all carriers present at x_m are produced by photoenhancement, the effect of the light intensity should not be strictly linear, but should be slightly less than linear. This is what is observed. The concentration of triplet excitons at x_m can be calculated, as was shown by Mulder,[20] to be

$$T(x_m) = \frac{2I_0 k l_T^2}{D(1 - k^2 l_T^2)}\left[\exp(-kx_m) - \exp\left(-\frac{x_m}{l_T}\right)\right] \tag{9}$$

where k is the absorption coefficient of the singlet exciton, and $l_T = \sqrt{D\tau_T}$; l_T is the diffusion length, τ_T is the lifetime, and D is the diffusion coefficient respectively of the triplet exciton. Let us assume for the moment (this will be substantiated in this section) that most of the triplet excitons lie within the potential well and that the average lifetime of the triplet excitons is determined almost entirely by the triplet quenching reaction $T + n_t \rightarrow S_0$. In other words,

$$\frac{1}{\tau_T} = \gamma_{Tt} n_t \tag{10}$$

or

$$\tau_T(\mathbf{0}) = (\gamma_{Tt}(\mathbf{0})n_t)^{-1}$$

where the designation (**0**) or (**H**) indicates either that there is no applied external magnetic field or there is a field of magnitude **H**, and γ_{Tt} is the magnetically sensitive (T–n_t) rate constant. The dependence of $(n_f)_{x_m}$ on **H** in equation (8) can be shown simply as

$$\frac{n_f(x_m; \mathbf{H})}{n_f(x_m; \mathbf{0})} = \frac{\gamma_{Tt}(\mathbf{H})T(x_m; \mathbf{H})}{\gamma_{Tt}(\mathbf{0})T(x_m; \mathbf{0})} \tag{11}$$

and the ratio $T(x_m; \mathbf{H})/T(x_m; \mathbf{0})$ can be derived from equations (9), (10), and the definition of l_T, to be

$$\frac{T(x_m; \mathbf{H})}{T(x_m; \mathbf{0})} = \frac{l_T^2(\mathbf{H})}{l_T^2(\mathbf{0})} \frac{1 - k^2 l_T^2(\mathbf{0})}{1 - k^2 l_T^2(\mathbf{H})} \left\{ \frac{\exp[-kx_m] - \exp[-x_m/l_T(\mathbf{H})]}{\exp[-kx_m] - \exp[-x_m/l_T(\mathbf{0})]} \right\} \tag{12}$$

where

$$l_T(\mathbf{H}) = \sqrt{D\tau_T(\mathbf{H})} = \sqrt{D/\gamma_{Tt}(\mathbf{H})n_t}$$
$$l_T(\mathbf{0}) = \sqrt{D\tau_T(\mathbf{0})} = \sqrt{D/\gamma_{Tt}(\mathbf{0})n_t}$$

For a value of $\gamma_{Tt}(\mathbf{0}) = 1.07\gamma_{Tt}(\mathbf{H})$,[24] one obtains $l_T(\mathbf{H}) = l_T(\mathbf{0})\sqrt{1.07}$. Using a reasonable value of $l_T(\mathbf{0}) = 0.3\mu$[17,19] and $k = 7 \times 10^4$ cm^{-1}, one obtains for equation (12) a ratio of 1.23 when x_m is about 2μ. There is thus a 23% increase in the triplet exciton density at x_m as a result of the magnetic field decoupling of the interaction of the triplet exciton with the trapped carrier in the potential well. With this result and equation (11), together with the data on the magnetic dependence of γ_{Tt},[24] one can obtain a net increase of 14% in the free carrier density at x_m which is in good agreement with the measured value of +14% in $\Delta J_{ph}/J_{ph}$ (see Figure 3c). In order for $\Delta J_{ph}/J_{ph}$ to be +14%, it is necessary that the triplet exciton lifetime be determined almost entirely by trapped carrier quenching. This imposes a lower limit to the density of trapped charge in the potential well. Taking the normal lifetime of the triplet exciton to be about 50×10^{-6}s,[17] it is required that $\gamma_{Tt}n_t \gg 2 \times 10^4$ s^{-1}. From the result of Kalinowski and Godlewski,[19] we have $\gamma_{Tt} \sim 5 \times 10^{-9}$ cm^{3}s^{-1}; thus $n_t \gg 4 \times 10^{12}$ cm^{-3}. From equation (6) we have calculated that n_a(total) $\simeq n_a$(trapped) $= 2.45 \times 10^{14}$ cm^{-3}. It is thus seen that these experimental results are self consistent.

An examination of Figure 3c shows that as V increases, the relative magnitude of $\Delta J_{ph}/J_{ph}$ decreases for $\lambda < \lambda_m$. The magnitude of $\Delta J_{ph}/J_{ph}$ for $\lambda < \lambda_m$ compared with that at $\lambda = \lambda_m$ decreases, and the peak to valley ratio in J_{ph} diminishes for $\lambda < \lambda_m$ (Figure 3a,b). All of these effects can be explained qualitatively by reference to the effect of V on the position of x_m. As V

increases, x_m decreases, eventually passing out of the crystal entirely as current saturation is reached. Thus, from equation (9) it can be shown that as x_m decreases, the relative number of triplet excitons that lie between $0 \lesssim x \lesssim x_m$ decreases as compared with those that lie between $x_m < x \lesssim L$. For example, for $x_m = 4l_T$ and a wavelength for which $1/k = x_m$, the ratio of the number of triplet excitons within the potential well to those outside of it is about 1; for $x_m = l_T/2$ under the same conditions, the ratio is 0.2. In other words, the triplet exciton population falls outside of the potential well as V increases. On the other hand, the ratio of the total number of singlet excitons in the potential well to those outside of it will remain constant, for $1/k = x_m$. Since the number of triplet excitons involved in detrapping in the region $x_m \lesssim x \lesssim L$ increases, and since $\Delta J_{ph}/J_{ph}$ is negative for this spatial region, the overall magnitude of $\Delta J_{ph}/J_{ph}$ should diminish, as it does. Furthermore, since the distribution of singlet excitons between the two regions of the crystal tends to be independent of V, for $1/k = x_m$, the detrapping role played by singlet excitons increases relative to the triplet excitons; this should make the peak to valley ratio in $\Delta J_{ph}/J_{ph}$ at $\lambda = \lambda_m$ (see Figure 3c) more nearly equal to that at $\lambda < \lambda_m$, as is the case. As for the weakened antibatic response at higher voltages seen in Figure 3b, this is a natural consequence of the fact that as x_m approaches l_T, the peak to valley ratio in the action spectrum should diminish.[20] Finally, as x_m and hence the potential passes out of the crystal, there should be no special role played by the singlet excitons, and the effect of the triplet excitons should dominate. This will be discussed in Section VIII.

VIII STATIONARY PEAK IN THE ACTION SPECTRUM AT HIGH VOLTAGE

As the external voltage is increased, the peak at λ_m moves towards shorter wavelengths, but eventually stops at some value λ'_m which is close to the main absorption peak. All things being equal, it is to be expected that x_m should eventually pass out of the crystal with increasing V and there seems to be no reason for the existence of a final value for λ'_m. However, in the surface region near to the anode, there is a greater concentration of trapping sites† (and hence of trapped carriers) than in the bulk. It is precisely in the surface region that a peak in the action spectrum for photoenhancement can be produced by the interaction of a high concentration of trapped carriers and an exciton distribution; we propose that the peak at λ'_m is

† The role played by the distortions in the surface region of the crystal in determining the triplet exciton lifetime has been described elsewhere.[30]

produced by such an interaction. The appearance of such a peak would mask the disappearance of x_m from the crystal, but this peak would be stationary with voltage and most important, should be consistent with the fact that there is no potential maximum lying at λ'_m.

The mechanism proposed for the apparently voltage independent peak in the photoenhancement action spectrum at λ'_m can be checked. Recall that at all previous values of λ_m, one observes a singlet exciton signature at x_m. If the peak at λ'_m is a result of the overlap of the exciton and trapped carrier distributions, and if there is to be no potential barrier at $1/k'_m$, then there should be no reason for singlet excitons to reveal themselves in the face of the preponderance of triplet excitons. In order to insure the vanishing of the potential barrier, the voltage must be increased until the current saturates. The determination of whether the contact is saturating is made easier if one notices the slope of the ln J vs ln V plot changing from the high value in the SCLC regime, to 1 in an ohmic region that precedes saturation, to less than 1 in the saturation region beyond the ohmic region (see p. 203, ref. 2). Such a transition was seen when Ce^{4+}(aqueous) electrodes were used,[31,32] but not when CuI electrodes were used. For example, in Figure 2, one notices that beyond 100 V, the slope of the ln J − ln V plot changes from a value (3.1) to a value (1.6). This indicates a trend towards an electrode limited current, but according to our hypotheses, the potential maximum is still inside the crystal at 200 V, and accounts for the results shown in Figure 4. Unfortunately, for this crystal, no lower voltage than 200 V was used for these measurements, but in another crystal, with identical contacts, a voltage in the region of large slope in the ln J vs ln V plot was used; the results were qualitatively the same as those shown in Figure 4.

Therefore, in order to insure that the actual current saturation region was being reached, we used the Ce^{4+}(aqueous) electrode. This saturation is a result of a diffusion limited rate of contact of Ce^{4+} ions with the tetracene surface.[33] With these Ce^{4+}(aqueous) electrodes, one observes the same movement of x_m with increasing V as is seen with CuI electrodes. In using a Ce^{4+}(aq) hole injecting electrode, we found that in the strictly saturated region, the magnetic effects were too small and noisy to measure accurately. We therefore selected a lower voltage V_c at which the current-voltage plot showed a distinct knee. At this voltage, a measurable magnetic effect was found. Other work in this laboratory[32] has shown that for voltages greater than V_c, the total space charge in the crystal decreases and is no longer linearly proportional to the voltage. At the voltage V_c, x_m should therefore be at the geometric anode, or at $x = 0$. However, at V_c, there is still space charge in the crystal, so there should still be a photoenhancement effect due to an increase in the ratio of free to trapped charge inside the crystal. The photocurrent should therefore increase if the concentration of excitons increases.

An external magnetic field decreases the concentration of singlet excitons in tetracene at low **H** and increases this concentration at high **H**.[22] The opposite effect is noted for the triplet exciton concentration, except that the maximum decrease in the triplet exciton population is expected to be less than 2%.[10] The effect of an external magnetic field on the photocurrent shown in Figure 6c is thus attributable to the triplet excitons; there is no sign of an appreciable singlet exciton contribution. The response shown in Figure 6c differs however from the normal triplet response in one important respect: the inversion takes place at 1100G instead of at 400G. To explain this increase in the

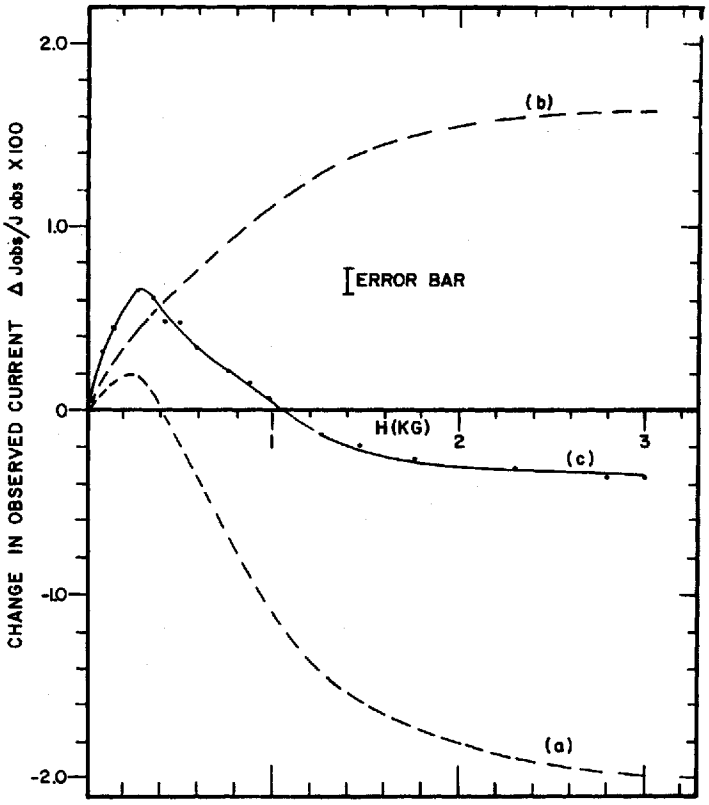

FIGURE 6a Hypothetical change in observed photocurrent if the change in the triplet exciton density were determined by the inhibition of singlet exciton fission by the external magnetic field.

FIGURE 6b Hypothetical change in observed photocurrent if the change in the triplet exciton density were determined by the inhibition of the T–n, quenching process.

FIGURE 6c Effect of an external magnetic field (at resonance position in the *ab* plane at an angle of 30° with respect to *b* axis) on the observed photocurrent in tetracene at onset of current saturation. $Ce(SO_4)_2$ (aqueous) anode, Ag cathode, 250 volts applied, $L = 180\mu$. $\lambda = 535$ nm $\| b$ axis, $l_a = 1/k = 0.4\mu$. For definition of J_{obs} see Appendix A.

inversion field strength, it is suggested that the result shown in Figure 6c is a resultant of two concurrent processes, shown schematically in Figure 6a and Figure 6b. In Figure 6a is seen the change in triplet exciton population that would be expected as a result of the inhibition of singlet exciton fission by the magnetic field.[15] In Figure 6b is seen the change in the photoinjection of free carriers at the surface by triplet excitons if their lifetime were to be *partially* determined by the T–n_t interaction in the bulk of the crystal; the external magnetic field inhibits the T–n_t interaction and therefore increases the number of triplet excitons at the surface where they dissociate to inject free carriers. The sum of the process 6a and 6b should approximate the observed results shown in Figure 6c.† In the voltage region used for Figure 6, just as in the case with CuI electrodes, one still observes the voltage independent peak at λ'_m.

The above agreements suggest that there is no potential barrier at λ'_m; there is instead a trapped charge distribution near the surface, with a center of gravity lying about 0.4μ from the geometrical surface. As for the crystal with the CuI electrode, with increasing V the slope drops from 3.1 to 1.6 in Figure 2; we attribute this to the beginning of the depletion of the carrier reservoir and hence to the beginning of the electrode limited current regime.

SUMMARY

Using tetracene crystals provided with hole injecting contacts CuI (solid) and $Ce(SO_4)_2$ (aqueous) we have located the position of the virtual anode x_m (potential maximum) within the crystal, and have followed its movement with applied voltage. For this purpose, we used the triplet and singlet exciton as tracers, making particular use of the characteristic response of these excitons to an external magnetic field. We have identified a peak at a wavelength λ_m in the long wavelength tail of the action spectrum of the photoenhanced current and we have taken $1/k_m$ as indicating the position of the potential maximum (x_m). As the external electric field is increased, x_m eventually passes out of the crystal and current saturation ensues. It appears that in all the cases that we have studied, the passage of x_m out of the crystal is masked by a local concentration of trapped charge in a region close to the surface of the crystal. It is remarkable that x_m appears to remain inside the crystal up to the onset of saturation. This behavior has been anticipated on theoretical grounds.[26] We have shown that the current dependence of x_m follows the simple form of the exact theory of current flow in insulators as proposed by Sinharay and Meltzer (SM). The SM theory is based on the assumption of a

† See Appendix A for a more detailed argument.

finite reservoir of free carriers at the injecting contact and hence at the virtual anode; highly absorbed light is instrumental in increasing the free carrier concentration at x_m. It is thus evident that a photoenhanced current can be produced not only by detrapping deep in the interior of the crystal, as proposed by Helfrich[6] but also by detrapping in the vicinity of x_m.

The peak at λ_m has been observed previously[12,13] and in particular, Bauser and Ruf have explained this peak in term of bulk detrapping, using the simple SCLC theory of Mark and Helfrich (MH). Although we can duplicate the mathematical form of the Bauser and Ruf expression without using their assumption, it is possible that our explanation and that of Bauser and Ruf are both correct, and that the apparent differences merely reflect the differences in the thickness of the crystals we both used.

One important consequence of our experiments is that by obtaining the spatial dependence of x_m as a function of the applied field, it becomes possible to provide measurable boundary conditions that in turn could facilitate the exact solution of the current-voltage dependence in insulators. With this solution, one could determine the field and charge distribution throughout the crystal, including the contact region.

Another result of these experiments is that we will be able to obtain quantitative comparisons of the carrier injecting efficiencies of various contacts.

It is also apparent that the use of the magnetic properties of excitons opens a new window into the study of the electrical properties of organic crystals. The importance of this technique is that it is effective at zero or low applied electric field as well as at high applied fields, whereas other techniques that depend on the electric field often encounter difficulties at the extremes in the electric field.

Acknowledgements

This work was supported by the National Science Foundation and the Atomic Energy Commission. We are grateful to Professor Dr. H. Kallmann for stimulating and valuable discussions. We are also grateful for the assistance given by Dr. S. Arnold, Professor N. E. Geacintov and Mr. J. Burgos.

References

1. N. Mott and R. Gurney, *Electronic Processes in Ionic Crystals*, Clarendon Press, Oxford, 1940, p. 169.
2. M. Lampert and P. Mark, *Current Injection in Solids*, Academic Press, New York, 1970.
3. G. T. Wright, *Solid State Electron.*, **2**, 165 (1961).
4. A. Rose, *Phys. Rev.*, **97**, 1538 (1955).
5. P. Mark and W. Helfrich, *J. Appl. Phys.*, **33**, 205 (1962).
6. W. Helfrich in *Physics and Chemistry of the Organic Solid State*, Vol. III, ed. by D. Fox, M. M. Labes, and A. Weissberger, Interscience Pub., New York, 1967, Chapter I.

7. N. Sinharay and B. Meltzer, *Solid State Electron.*, **7**, 125 (1964).
8. N. Sinharay, *Ph.D. Thesis*, Edinburgh University, 1963.
9. M. Pope, S. Fox, and N. Geacintov in *Organic Scintillators and Liquid Scintillators Counting*, ed. by D. L. Horrocks and C. T. Peng, Academic Press, 1971, p. 489.
10. S. Fox, *Ph.D. Thesis*, New York University, 1969.
11. R. I. Frank and J. G. Simmons, *J. Appl. Phys.*, **38**, 832 (1967).
12. H. Bauser and H. H. Ruf, *Phys. Stat. Sol.*, **32**, 135 (1969).
13. T. Asada, K. Sugihara, Y. Kimura, and S. Owaki, *Mem. Inst. Sci. & Ind. Res.*, Osaka University, **22**, 89 (1965).
14. G. Vaubel and H. Baessler, *Mol. Cryst. and Liq. Cryst.*, **12**, 47 (1970).
15. M. Pope, N. Geacintov, and F. Vogel, *Mol. Cryst. and Liq. Cryst.*, **6**, 83 (1969).
16. R. Alfano, S. Shapiro, and M. Pope, *Opt. Commun.*, **9**, 388 (1973).
17. M. Pope, N. E. Geacintov, D. Saperstein, and F. Vogel, *J. Luminescence*, **1**, 224 (1970).
18. G. Vaubel and H. Kallmann, *Phys. Stat. Sol.*, **35**, 789 (1969).
19. J. Kalinowski and J. Godlewski, *Phys. Stat. Sol.*, **20**, 403 (1973).
20. B. J. Mulder, *Phys. Res. Rept. Suppl.* No. 4, 1968.
21. C. E. Swenberg and W. T. Stacy, *Chem. Phys. Rev. Lett.*, **2**, 327 (1969).
22. N. E. Geacintov, M. Pope, and F. Vogel, *Phys. Rev. Lett.*, **22**, 593 (1969).
23. P. Avakian and R. E. Merrifield, *Mol. Cryst.*, **5**, 37 (1968).
24. V. Ern and R. E. Merrifield, *Phys. Rev. Lett.*, **21**, 609 (1968).
25. N. E. Geacintov, M. Pope, and S. Fox, *J. Phys. Chem. Sol.*, **31**, 1375 (1970).
26. H. Kallmann (private communication).
27. M. Schott and J. Berrihar, *Mol. Cryst. and Liq. Cryst.*, **20**, 13 (1973).
28. V. Ern, H. Bouchriha, J. Fourny, and G. Delacote, *Solid State Comm.*, **9**, 1201 (1971).
29. H. Baessler, G. Herrmann, N. Riehl, and G. Vaubel, *J. Phys. Chem. Sol.*, **30**, 1579 (1969).
30. M. Pope and H. Kallmann, *Israel Journ. Chem.*, **10**, 269 (1972).
31. M. Pope, H. Kallmann, A. Chen, and P. Gordon, *J. Chem. Phys.*, **36**, 2486 (1962).
32. M. Pope and W. Weston, *Mol. Cryst. and Liq. Cryst.*, **25**, 205 (1974).
33. W. Mehl, *Ber. Bunsenges Physik Chem.*, **69**, 583 (1965).
34. A. Bree and L. E. Lyons, *J. Chem. Soc.*, 5206 (1960).
35. E. L. Frankevich and J. A. Sokolik, *Sov. Phys. Sol. State*, **9**, 1532 (1968).

Appendix A

Just before the potential maximum leaves the crystal, and the current saturation region is entered, the observed current J_{obs} tends to become ohmic,[32] i.e. $J_{obs} \simeq n_f e\mu V/L$. In this narrow voltage range, the photo-enhanced response is still antibatic, indicative of a process of detrapping of carriers by triplet excitons from a region deeper into the crystal. In this voltage range, the photoinjection of carriers by the dissociation of triplet excitons at the surface becomes more important than in the case when the potential maximum is present in the bulk of the crystal, and the concentration of carriers in the reservoir at the anode is large. The effect of a magnetic field should reduce the detrapping process and hence cause $\Delta J_{ph}/J_{ph}$ to be negative for all values of **H**. The addition of a negative $\Delta J_{ph}/J_{ph}$ to the curve shown in Figure 6a (i.e. the change in the triplet population as a function of **H**) would shift the inversion point from its normal value at 400G to

lower values; instead, one sees that the inversion point lies at 1100G. One must therefore conclude that although the antibatic response and the magnetic effect are due to triplet exciton dynamics, there must be a rather subtle combination of processes involved.

A proposed explanation of the experimental results is as follows: In the voltage range where SCLC are measured, there is a large and adequate reservoir of carriers at the injecting Ce^{4+} electrode. Since the currents that flow do not make a great demand on the reservoir, it does not matter whether the reservoir is enlarged by exciton dissociation at the surface. Thus, in the SCLC range, exciton dissociation has a minor effect on the total current flowing, and only detrapping in the bulk can increase the current; J_{ph} is therefore the only current that is relevant. However, at higher voltages, the reservoir is depleted, and in this case, the total current is the sum of the current produced by Ce^{4+} injection and exciton dissociation. Consider therefore that the observed photocurrent (J_{obs}) is the sum of two independent processes. These are

$$J_{obs} = J_{ph} + J_{pi} \tag{A-1}$$

where J_{ph} is the photoenhanced current produced by the detrapping of carriers in the bulk and J_{pi} is the additional current produced by the dissociation of triplet excitons at the Ce^{4+} surface. In the voltage range for this experiment where $J_{obs} \simeq n_f e\mu V/L$, the photoenhancement would be due to an increase in n_f in the bulk. We assume that $J_{ph} > J_{pi}$ and therefore, that J_{obs} would show an overall antibatic response, as indeed it does. It must now be shown that the magnetic response $\Delta J_{obs}/J_{obs}$ can be due mainly to J_{pi}. In other words, we propose that the magnetic effect in this voltage range singles out the photoinjection process, while the action spectrum for J_{obs} singles out the detrapping process. Thus, from equation (A-1), it can be shown that the desired relation is

$$\frac{\Delta J_{pi}}{J_{pi}} > \frac{J_{ph}(0)}{J_{pi}(0)} \cdot \frac{\Delta J_{ph}}{J_{ph}} \tag{A-1a}$$

where $\Delta J_{pi} \equiv J_{pi}(H) - J_{pi}(0)$. Since $J_{ph}(0) > J_{pi}(0)$, it is necessary that $\Delta J_{ph}/J_{ph}$ be small enough to insure the validity of equation (A-1a).

The photoinjection process depends linearly on the flux of triplet excitons reaching the surface which in turn depends linearly on the concentration of triplet excitons at every point x inside the crystal.[20]

As for J_{ph}, this current is due to detrapping process in which $J_{ph} \propto n_f$, and n_f is determined by the following T–n_t interaction:

$$\frac{d[T]}{dt} = g - [T](k_T + \gamma_{Tt} n_t) = g - \frac{[T]}{\tau'_T} = 0 \tag{A-2}$$

where

$$\frac{1}{\tau'_T} = (k_T + \gamma_{Tt} n_t)$$

$$\frac{dn_t}{dt} = \gamma_{ft} n_f N_t - k_{th} n_t - \gamma_{Tt}[T] n_t = 0 \tag{A-3}$$

where g is an overall generation rate for triplet excitons; k_T is the monomolecular decay rate for triplet excitons, and includes the effect of surface quenching when the excitons are generated within a diffusion length of the surface, and τ'_T is the effective lifetime of the triplet exciton; γ_{ft}, N_t and k_{th} are respectively the trapping rate for free carriers, the density of unfilled trapping sites, and the thermal detrapping rate of trapped carriers. Under steady state conditions, the concentration of free carriers, n_f, is to be taken to be due mainly to the photoenhanced process, as is implied by the antibatic action spectrum of J_{ph} and the fact that the photoenhanced current is about two times larger than the dark current. From equations (A-2) and (A-3) one obtains

$$[T] = g/(k_T + \gamma_{Tt} n_t) = g\tau'_T \tag{A-4}$$

and

$$n_f = n_t(k_{th} + \gamma_{Tt}[T])/\gamma_{ft} N_t \tag{A-5}$$

Inserting equations (A-4) into (A-5), one obtains

$$n_f = \frac{n_t}{\gamma_{ft} N_t}(k_{th} + g\gamma_{Tt}/(k_T + \gamma_{Tt} n_t)). \tag{A-6}$$

Since $J_{ph} \propto n_f$, it can be seen from equation (A-6) that the magnetic dependence of J_{ph} derives only from the term γ_{Tt}. If k_{th} is very large, then the magnetic effect is expected to be insignificant. However, if this were the case, the photoenhancement effect would be very small, which is not the case, so k_{th} cannot be the source of the weak magnetic dependence of J_{ph}. Referring once more to equation (A-6), if $\gamma_{Tt} n_t \gg k_T$, then there will be no magnetic dependence at all for J_{ph}. However, looking at equation (A-4), if $\gamma_T n_t \gg k_T$, then the effective lifetime of the triplet exciton would be determined by $\gamma_{Tt} n_t$, and there should be a 7% increase in τ'_T in the presence of a saturation value of **H**. It can be shown in a manner similar to that shown in equation (12) that the net result of this increase in τ'_T would be to make the value of $\Delta J_{pi}/J_{pi}$ in Figure 6b positive for all values of **H**. It must therefore be concluded that $k_T \simeq \gamma_{Tt} n_t$, which is not unreasonable, since the concentration of trapped carriers must diminish as current saturation is entered. From equations (A-4) and (A-6), going through the necessary algebra, one can derive, (neglecting for the moment the fact that g is also magnetically sensitive

since it depends on the singlet exciton fission process)

$$\frac{\Delta T/T}{\Delta n_f/n_f} = -\frac{\gamma_{Tt}(0)n_t}{k_T}\left\{1 + \frac{k_{th}n_t}{g}\left(1 + \frac{k_T}{\gamma_{Tt}(0)n_t}\right)\right\} \simeq \frac{\Delta J_{pi}/J_{pi}}{\Delta J_{ph}/J_{ph}} \quad \text{(A-7)}$$

where the Δ's refer as usual to the changes due to the applied magnetic field. The condition required in equation (A-1a) demands certain relationships among the quantities in equation (A-7). It can be shown that equation (A-7) implies that the absolute value

$$\left|\frac{\Delta J_{pi}/J_{pi}}{\Delta J_{ph}/J_{ph}}\right| > \frac{\gamma_{Tt}(0)n_t}{k_T} \quad \text{(A-8)}$$

Therefore, if $\gamma_{Tt}(0)n_t \gtrsim k_T$, we can satisfy equation (A-1a). The attainment of equation (A-8) will generate the curve in Figure 6b, and the additional magnetic effect on g in equation (A-7) generate the curve in Figure 6a. In fact, it can be predicted that at higher voltages than 250 volts, the curve in Figure 6c will look more and more like Figure 6a because n_t diminishes, eliminating the role of detrapping, and emphasizing the role of photoinjection; the action spectrum for the photoenhanced current should become accordingly more symbatic. In another crystal bearing a Ce^{4+} electrode, this type of transition has been observed.

The picture that emerges is therefore that as the current saturation region is entered and the potential maximum passes out of the crystal, the triplet exciton concentration becomes less dependent on T–n_t interactions, and photoinjection becomes more important. However, when the potential maximum is inside the crystal, and $\gamma_{Tt}n_t \gg k_T$, an external magnetic field has no effect on n_f within the potential well (see Section VII) but does have its maximum effect in increasing $[T]$ through equation (A-4): This produces the increased concentration of triplet excitons at x_m with the accompanying magnetic dependence as described in Section VII.

Thus, with increasing applied voltage, x_m passes out of the crystal, the density of trapped carriers diminishes, and the effects described in Section VIII appear.